8th International Symposium on Magnetic Bearing
August 26-28, 2002, Mito, Japan

NONLINEAR STATE CONTROL OF A LEFT VENTRICULAR ASSIST DEVICE (LVAD)

Christian Huettner
Electrical Engineering and Design Laboratory, Swiss Federal Institue of Technology Zurich,
8005 Zurich, Switzerland
huettner@eek.ee.ethz.ch

ABSTRACT

Implantable left ventricular assist devices are powered by batteries; their limited capacity has to be used as efficiently as possible. It was demonstrated on the example of a MAGLEV centrifugal LVAD that by designing an optimized controller a remarkable reduction of power consumption could be achieved, especially for transient disturbances. The key concept is the combination of exact linearization to decouple the system and the application of adaptive vibration control. The potential benefits of the nonlinear controller are discussed.

INTRODUCTION

The rotor of the Bearingless Slice Motor is a two pole permanent magnet with an almost sinusoidal field distribution. A detailed description of the application can be found in [15] and [16]. Any eccentricity (we face a large air-gap magnetic bearing, see [14]) of the rotor causes nonlinear force distributions, which have to be considered in the design of a suitable controller. The forces vary with the magnitude of the eccentricity and also depend on the angular position of the rotor. Furthermore these forces cause an angular dependant coupling with coupling forces achieving up to 50% of the desired or applied force. The discussed coupling arises from the specific setup consisting of the permanent magnet and the disc shaped rotor. It is therefore desired to eliminate the nonlinearity to obtain a model with constant stiffness and no coupling forces. This is the purpose of a decoupling controller which compensates the interconnections of the multivariable (MIMO) system in such a way, that the overall system then behaves like two decoupled single input - single output (SISO) systems. The decoupling controller is expected to be robust against parameter changes to ensure success in an industrial application.

The field of decoupling controllers has been investigated for a long time(see [2] and [7]); for magnetic bearings i.e. [1]; in [3] a modal decomposition of the differential equations is proposed. A key issue why nonlinear control is applied in an increasing number of applications is to have a constant system performance across a large operational area. Since in the considered case the nonlinearity affects the stiffness of the plant depending on the angular rotor position, no local linearization is applicable. Furthermore the nonlinear coupling could not be compensated by any decoupling strategy. Decoupling can also be achieved through feedback linearization. For the theory concerning the exact linearization method for MIMO systems the reader is referred to [6], [12], [13] and [18]. Since we face a strong nonlinear coupled system, we can expect the nonlinear decoupling controller to be more efficient than a controller designed for any linearized model. The exact linearization method has been applied to magnetic bearings several times, see i.e. [11] and [17]. Multivariable state feedback in our case is necessary; nonmeasureable state information is provided by an observer. In [9] Kawanishi states, that in MIMO-treated active magnetic bearing systems, considering rotor dynamics, input-state linearization technique cannot be applied due to the complexity of the model. In our case input-output exact linearization technique is applicable. The reference controller (the former design) is a tuned and optimized PID position controller with an underlying PI current controller designed for independent SISO (single input- single output) systems. It reacts onto coupling forces as if they were independent disturbance forces. In order to apply optimal controller outputs the angle of the rotor also has to be an input parameter of the new controller, but not only for coordinate transformations as it was for the former controller design. Numerical simulations

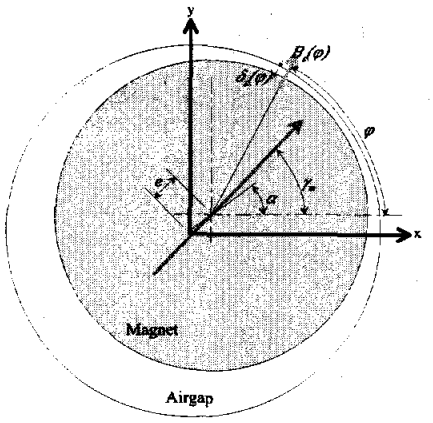

FIGURE 1: Unbalance Force

are presented to demonstrate the optimal nonlinear implementation. Measurements on the implantable blood pump illustrate the effectiveness of the proposed controller in the last section.

NONLINEAR MODEL

The rotor of the bearingless slice motor is a permanent magnet with two poles ($p = 1$, with p being the number of polepairs). No unbalance is assumed which equals to no forces acting on the rotor in center position ($e = 0$). A rotor displacement off center (see Figure 1) ($e \neq 0$) causes an additional force. The magnetic induction B depending on the angle φ and on the orientation (and γ_m indicating the direction of magnetization) can be described as:

$$B_0(\varphi) = \widehat{B} \cdot cos(p\varphi - \gamma_m) \tag{1}$$

The airgap depending on the eccentricity and on the angle (see [8]) can, in a simplified way, be explained as:

$$\delta_\varepsilon(\varphi) = \delta_0 - e \cdot cos(\alpha - \varphi) \tag{2}$$

The magnetic induction depending on the airgap δ_0 (and with l_{PM} the rotor radius) leads to:

$$B_\varepsilon(\phi) = B_0(\varphi)\frac{l_{PM} + \delta_0}{l_{PM} + \delta_\varepsilon} \tag{3}$$

After the integration (for $p = 1$) of the differential force, and some straightforward calculations (see [4]) the force acting on the rotor emerges to:

$$\vec{F} = k_s \cdot (\boldsymbol{I} + c_s \boldsymbol{C}) \cdot \begin{bmatrix} x \\ y \end{bmatrix} \tag{4}$$

where

$$\boldsymbol{C} = \begin{bmatrix} \cos(2\gamma) & \sin(2\gamma) \\ \sin(2\gamma) & -\cos(2\gamma) \end{bmatrix} \tag{5}$$

with k_S denoting the stiffness of the magnetic bearing and c_S being the coupling parameter between the two axes x and y. Note: Coupling here only occurs for $p = 1$. As visible in the arguments on the harmonic functions a π-periodic component arises for $c_S \neq 0$ which is the source of the nonlinearity considered in this paper.

Extension of Model

The derived additional force component has to be taken into consideration for getting a model of the bearing. Equation 4 consists of two components in the feedback path of the bearing model: a constant, a well known one, the stiffness k_S of the bearing and another one, the γ-dependant part. This matrix can further be split into two components: the diagonal ($c_S k_S cos(2\gamma_S)$) blocks for stiffness variation and the non-diagonal ($c_S k_S sin(2\gamma_S)$) blocks for coupling. The first one adds to the bearing stiffness k_S and the latter is the source of the axial interaction and can be seen as an additional disturbing force. Figure 2 shows the influence of equ. 4 on the model for the two-axis magnetic bearing[1].

Description of the Model

Several nonlinear effects which occur in the investigated magnetic bearing are not considered:

- The force-current characteristic is assumed to be linear and independent of the rotor position as well as the natural stiffness for a *fixed* angle. $f_{mag} = k_i \cdot i + k_x \cdot x$
- Position sensing is assumed to be linear in the area of interest
- The power converters are treated as ideally fast.
- The rotor is 2-pole sinusoidal magnetized and has no unbalance
- $\boldsymbol{R}$ and $\boldsymbol{L}$ are constant and independent of the air gap
- All electromagnets are identical

The focus of this paper is on the angular stiffness and on the coupling dependency. The (bearing) model derived above is described in equ. 6. The motor part is omitted, since it follows standard design procedures. ω and γ remain states. For transparency purposes two simplifications have to be made: Use the approximations for $\boldsymbol{R}$ and $\boldsymbol{L}$ mentioned below and set $\boldsymbol{C_i} = 0$, which means that iron core saturation effects are not considered in the model.

[1] The same coupling and parameter variation is applicable and occurs for the forward path for the multiplication with k_i in the model but is of a significantly less influence. C_i is of the same structure as C_s.

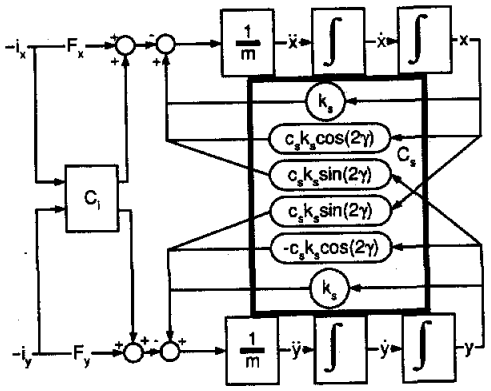

FIGURE 2: Bearing Model

$$i = [i_d\ i_q\ i_m]^T \quad \xi = [x\ y\ \gamma]^T \quad \dot{\xi} = [v_x\ v_y\ \omega]^T$$

$$\boldsymbol{L} = \begin{bmatrix} L_{11} & L_{12} & L_{13} \\ L_{21} & L_{22} & L_{23} \\ L_{31} & L_{32} & L_{33} \end{bmatrix} \quad \text{where } L_{ij} \approx 0 \text{ for } i \neq j \text{ and } L_{11} = L_{22}$$

$$\boldsymbol{R} = \begin{bmatrix} R_{11} & R_{12} & R_{13} \\ R_{21} & R_{22} & R_{23} \\ R_{31} & R_{32} & R_{33} \end{bmatrix} \quad \text{where } R_{ij} \approx 0 \text{ for } i \neq j \text{ and } R_{11} = R_{22}$$

where i: currents in coils, ξ: position of rotor $\dot{\xi}$: speed components.

$$\dot{x} = f(x) + g(x) \cdot u \quad y = h(x) \tag{6}$$

where $x \in \Re^n$ is the state vector, $f(x)$ and $g(x)$ are real smooth vector fields on $\Re^n$, and u is the control input.

$$g(x) = \boldsymbol{L^{-1}} \cdot u \tag{7}$$

$$\frac{\partial}{\partial t} i = -\boldsymbol{L^{-1}R} \cdot i - \boldsymbol{L^{-1}} k_i \cdot \dot{\xi} + g(x) \cdot u \tag{8}$$

$$\frac{\partial}{\partial t} \xi = \boldsymbol{I} \cdot \dot{\xi} \tag{9}$$

$$\frac{\partial}{\partial t} \dot{\xi} = \frac{k_i}{m} (\boldsymbol{I} + c_i \boldsymbol{C}) \cdot \begin{bmatrix} i_d \\ i_q \end{bmatrix} + \frac{k_s}{m} (\boldsymbol{I} + c_s \boldsymbol{C}) \cdot \begin{bmatrix} x \\ y \end{bmatrix} + \frac{p}{J} i_m \tag{10}$$

The focus of the presented model description is on the bearing, the drive model is straight forward, all nonlinearities except magnetic forces are neglected.

AI LINEARIZATION

The system is exactly linearizable. Exact input-output linearization considering the dynamics is applied on the MIMO (multiple input-multiple output) system and enables the decoupling of the system. The system is then fully independent of the rotational speed and the angular position. The theory of exact linearization is covered by many other publications and, as mentioned, omitted here. Applying the algorithms described in [10] to the nonlinear model described in equ. 6 one obtains the feedback law equ. 12. It consists of two parts: the internal feedback and a new control variable v_{in}.

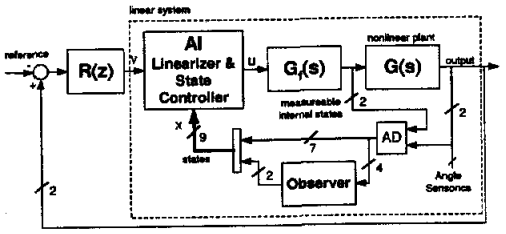

FIGURE 3: Linearized Model

$$u = \begin{bmatrix} u_d \\ u_q \end{bmatrix} = \alpha(x) + \beta(x) \cdot v_{in} = \tag{11}$$

$$= \begin{bmatrix} \alpha_d(x) \\ \alpha_q(x) \end{bmatrix} + \beta(x) \cdot \begin{bmatrix} v_{d,in} \\ v_{q,in} \end{bmatrix} \tag{12}$$

$$\sigma_C = k_s c_s \cos(2\gamma) \quad \sigma_S = k_s c_s \sin(2\gamma) \tag{13}$$

$$\beta(x) = \begin{bmatrix} \frac{ml}{k_i} \\ \frac{ml}{k_i} \end{bmatrix} \tag{14}$$

$$\begin{aligned} \alpha_d(x) = {} & (R_{11} - L_{11} \cdot a_{12}) \cdot i_d \\ & -\tfrac{L_{11}}{k_i} (m \cdot a_{10} + a_{12} (k_s + \sigma_C)) \cdot x \\ & +\tfrac{L_{11}}{k_i} \sigma_S \cdot y \\ & \left(k_i - \tfrac{L_{11}}{k_i} (m \cdot a_{11} + k_s + \sigma_C)\right) \cdot v_x \\ & -\tfrac{L_{11}}{k_i} \sigma_S \cdot v_y \\ & +2\tfrac{L_{11}}{k_i} \sigma_S \cdot \omega \\ & -2\tfrac{L_{11}}{k_i} \sigma_C \cdot y \cdot \omega \end{aligned} \tag{15}$$

$$\begin{aligned} \alpha_q(x) = {} & (R_{22} - L_{22} \cdot a_{22}) \cdot i_q \\ & +\tfrac{L_{22}}{k_i} \sigma_S \cdot x \\ & -\tfrac{L_{22}}{k_i} (m \cdot a_{20} + a_{12} (k_s - \sigma_C)) \cdot y \\ & -\tfrac{L_{11}}{k_i} \sigma_S \cdot v_x \\ & \left(k_i - \tfrac{L_{22}}{k_i} (m \cdot a_{21} + k_s - \sigma_C)\right) \cdot v_y \\ & +2\tfrac{L_{22}}{k_i} \sigma_S \cdot \omega \\ & -2\tfrac{L_{11}}{k_i} \sigma_C \cdot x \cdot \omega \end{aligned} \tag{16}$$

The MIMO system now consists of the two new transfer functions $G_{ax} = \frac{1}{s^3 + a_2 s^2 + a_1 s + a_0}$ for the x and y-axis if $a_{1i} = a_{2i}$ which is reasonable for this symmetric system. The values for a_i may arbitrarily be chosen. A superior controller has to be designed for a plant described in equ. 17, with the control input v_{in}. In a specific case, where the reference value remains constantly zero, it might be possible

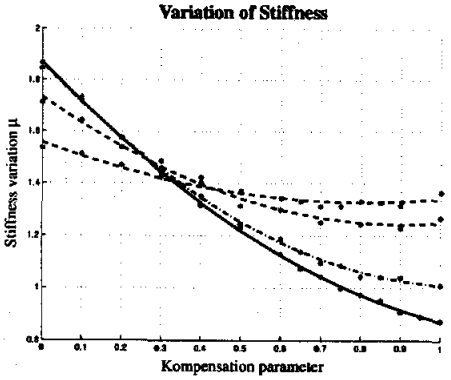

FIGURE 4: Stiffness Linearization

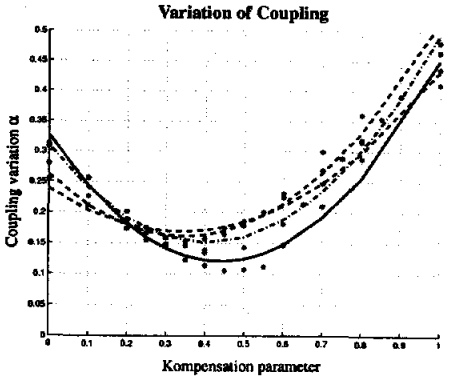

FIGURE 5: Coupling Compensation

to omit any superior controller. This increases the necessity of well chosen values for a_i.

$$G_{cl} = \begin{bmatrix} \frac{1}{s^3+a_2s^2+a_1s+a_0} & 0 \\ 0 & \frac{1}{s^3+a_2s^2+a_1s+a_0} \end{bmatrix} \quad (17)$$

CONTROLLER DESIGN

We still need to choose reasonable values for a_i. If $c_s = 0$, we have a linear SISO system. The resulting feedback can be seen in equ. 18 for the x-axis which is the same as equ. 19 for the y-axis.

$$\begin{aligned} \alpha_{dL}(x) = \quad & (R - L \cdot a_2) \cdot i_d \\ & -\tfrac{L}{k_i}(m \cdot a_0 + a_2 k_s) \cdot x \\ & \left(k_i - \tfrac{L}{k_i}(m \cdot a_1 + k_s)\right) \cdot v_x \end{aligned} \quad (18)$$

$$\begin{aligned} \alpha_{qL}(x) = \quad & (R - L \cdot a_2) \cdot i_q \\ & -\tfrac{L}{k_i}(m \cdot a_0 + a_2 k_s) \cdot y \\ & \left(k_i - \tfrac{L}{k_i}(m \cdot a_1 + k_s)\right) \cdot v_y \end{aligned} \quad (19)$$

We have a simple state controller with the feedback law described in equ. 20 and 21.

$$K_{SC} = [\kappa_{curr}\ \kappa_{pos}\ \kappa_{vel}]^{-1} \quad (20)$$

$$\begin{aligned} \kappa_{curr} &= -R + L \cdot a_2 \\ \kappa_{pos} &= \tfrac{L}{k_i}(m \cdot a_0 + a_2 k_s) \\ \kappa_{vel} &= \tfrac{L}{k_i}(m \cdot a_1 + k_s) - k_i \end{aligned} \quad (21)$$

There remains the discussion of designing a feedback controller to obtain optimal values for the parameters a_i. Applying standard LQ-design with the cost function

$$J = \frac{1}{2}\sum_{k=0}^{N}\left(x^T(k)\,\boldsymbol{Q}x(k) + u^T(k)\,\boldsymbol{R}u(k)\right) \quad (22)$$

results in the Riccati equation

$$P = \boldsymbol{Q} + \boldsymbol{A}^T P(\boldsymbol{A} - \boldsymbol{B}K) \quad (23)$$

with

$$K = \left(\boldsymbol{R} + \boldsymbol{B}^T P \boldsymbol{B}\right)^{-1} \boldsymbol{B}^T P \boldsymbol{A} \quad (24)$$

as the solution. $\boldsymbol{A}$ and $\boldsymbol{B}$ being the system matrices of the linear ($c_s = 0$) system. The translational speed in the plane of the disc is observed by a Kalman observer. As a superior controller there was simply chosen an integrator. The obtained control voltages are in rotor frame and need to be transferred into a stator fixed coordinate system.

Single Fault Tolerance

The industrial application, the controller is designed for, is single fault tolerant. Single fault tolerance requires a further extension of the control strategy: Fault handling routines have to ensure a linear signal path to avoid any discontinuities.

Adaptive Vibration Control

Additionally vibration control algorithms are running on the blood pump. While the control algorithms presented above focus on transient disturbances and hence reduce the energy consumption, vibration control deals with much larger time constants. The achievable benefit was further discussed in [5].

EXPERIMENTAL EVALUATION

Simulations have been carried out to compare the feedback controller design under many different conditions with the reference controller. After implantation the controller has to withstand many different challenging load conditions. For this reason the feedback controller design was tested under numerous conditions. A few results can be presented here. Figure 4 displays the achievable linearization for four

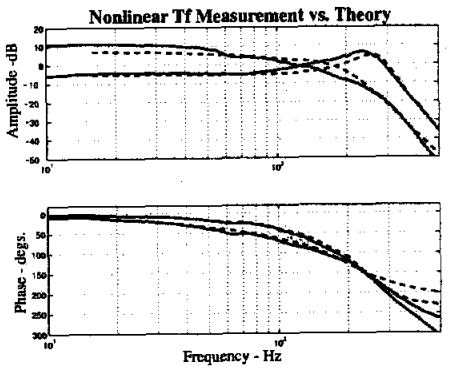

FIGURE 6: Transfer function without Comp.

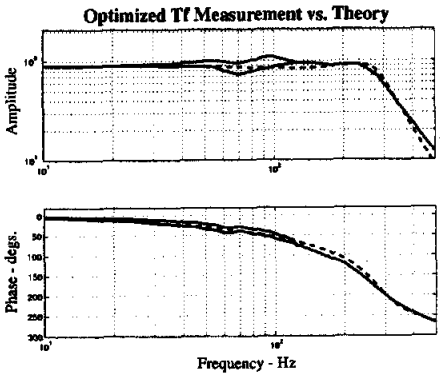

FIGURE 7: Transfer function after Compensation

frequencies 40, 50, 60 and $80Hz$. Depending on an additionally introduced parameter (κ_s, x-axis in plot) the compensation performance can be monitored and optimized. With $c_s = 0.25$ the variation between maximum and minimum stiffness is $1.7\left(=\frac{1+c_s}{1-c_s}\right)$ and can be reduced to the ideal and full compensation $1\,(=c_s=0)$ for the lower and to about 1.2 for the higher frequencies for $\kappa_s = 0.75$. The other measure of linearization performance is decoupling, displayed in Figure 5. With $c_s = 0.25$ again we have 0.25 coupling force for no compensation, or $\kappa_c = 0$. In practice an almost decoupling (which is frequency dependant) can be achieved (ideally 0, which means no coupling force, hence full decoupling). Now c_s can be reduced to about 0.1 for lower and about 0.15 for higher frequencies, with the optimum for $\kappa_c = 0.45$. Both parameters, κ_s and κ_c are in practical use close to the theoretically derived values.

Besides measuring the effects one wants to achieve directly (like energy reduction), another reasonable tool to prove the effectiveness of the linearization is the transfer function measurement. Figure 6 shows the comparison between the theoretical (dashed curves) and the measured transfer function (solid curves), for the two extremes. One measurement was done for maximum stiffness; the measurement was averaged for four positions (0, x-excitation; $\frac{\pi}{2}$, y-excitation; π, x-excitation and $\frac{3}{2}\pi$, y-excitation) to eliminate any dissymmetry in the setup. The maximum error does not go beyond $2dB$, which is mainly due to measurement errors than to model uncertainties. According to this the measurements for minimum stiffness were done. After compensation one obtains Figure 7. Again comparisons between the theory and the measurements are displayed for the minimum and the maximum stiffness. Apart from the frequency range $60-80Hz$ where a $2dB$ difference could not be eliminated, almost exact compensation was achieved. The other effect besides linearization is decoupling which is displayed in Figure 8. Considerable reduction in coupling forces could especially be achieved for the lower frequencies and were still satisfying in the frequency of the major point of operation. The dashed graphs are the direct transfer function (upper, i.e. x vs. x) and coupling for angle 0, which corresponds to no coupling. The two solid lines represent coupling before (upper) and after (lower) compensation. This equals an improvement of up to $40dB$.

Considerations about robustness against parameter variations also were done but are omitted in this paper. Power reductions in percentage were difficult to obtain. The magnetic forces are sources for the second harmonic which can be compensated by vibration control. These forces are the main reason for compensation and hence for an achievable benefit out of the presented control strategy. Therefore, with vibration control turned off, the possible power reduction is highest. It reaches, depending on the disturbances, load conditions, rotational speed, medium to be pumped as well as setup and impeller, up to 25%. It can averagely be stated, that with vibration control turned on [2], a reduction in energy consumption of 5% to 15% can be achieved.

SUMMARY

Exact linearization method was applied to a disc shaped rotor. With this, linearizing feedback controller measurements, especially for transient disturbances but also long term measurements were done to verify and prove the capability of the controller based on the linearization technique. The decrease in power consumption is shown and discussed. Measurements showed no interference or unwanted interaction between the position and vibration control. For example, step responses are now independent of the angular rotor position and the plant acts now in

[2]This is the only case with practical relevance for this application. For other bearingless slice motor applications with the same behavior in the transfer function the same control strategy might be applied without vibration control.

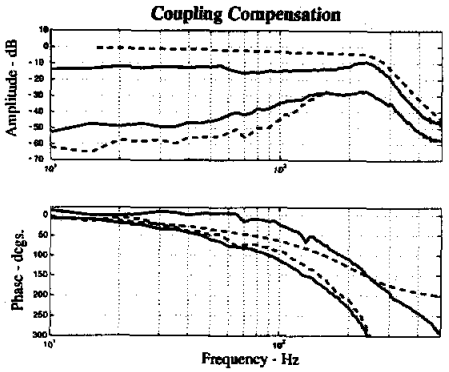

FIGURE 8: Coupling with / without compensation

a decoupled way. Future activities will focus on additional simplification and adaptation of the algorithm for a further improvement of performance.

References

1. Aeschlimann B., Model Based Decoupling Control of a Disc Rotor on Active Magnetic Bearings, Proc. of the 7th Int. Symp. on Magnetic Bearings, ETH Zurich, Aug. 2000.
2. Falb, P., Wolovich, W., Decoupling in the Design and Synthesis of Multivariable Control Systems, IEEE Trans. on Automatic Control Vol. AC-12, No. 6, Dec. 1967.
3. Hilton, E.F., Allaire, P. et al, Magnetic suspension test controller for a new continous flow ventricular assist device. Proc. of the 6th Int. Symp. on Magnetic Bearings, MIT Cambridge, USA, 1998.
4. Huettner, C., Analysis and Simulation of a Magnetic Synchronous Disc Motor, Diploma Thesis, Johannes Kepler University of Linz, Mar. 1999.
5. Huettner, C., Adaptive Vibration Control in an Implantable Blood Pump on a Bearingless Slice motor, Proc. of the 6th Int. Conf. on Motion and Vibration Control, Saitama, Japan, Aug. 2002.
6. Isidori, A., Nonlinear Control Systems, Springer Verlag, Third Edition, 1994.
7. Janiszowski, K., Unbehauen, H., Entwurf eines neuartigen diskreten Entkopplungsreglers fuer Mehrgroessenregelstrecken, Automatisierungstechnik at (german), 35. Jahrgang, Vol. 2, 1987.
8. Jaenicke, P., Die Berechnung der elektro magnetischen Zugkraefte bei Drehstrom synchronmaschinen mit statischer Exzentrizitaet, Dissertation, Technische Universitaet Hannover, 1975.
9. Kawanishi, M., Kanki, H., AMB Nonlinear Control with input-output exact linearization considering modal characteristics, Proc. of the 7th Int. Symp. on Magnetic Bearings, ETH Zurich, Aug. 2000.
10. Kugi, A., Schlacher K. and Novak, R., Symbolic Computation for the Analysis and Synthesis of Nonlinear Control Systems, Software for Electrical Engineering, Analysis and Design IV, A. Konrad and C.A. Brebbia (eds.), WIT-press, pp.255-264, 1999.
11. Namerikawa, T., Fujita, M. and Matsumura, F., Wide Area Stabilization of a Magnetic Bearing using Exact Linearization, Proc. of the 6th Int. Symp. on Magnetic Bearings, MIT Cambridge, USA, 1998.
12. Nijmeijer, H. and van der Schaft, A.J., Nonlinear Dynamical Control Systems, Springer Verlag, 1990.
13. Marino, R. and Tomei, P., Nonlinear Control Design, Prentice Hall, 1995.
14. de Queiroz, M.S., Dawson, D.M. and Suri, A., Nonlinear Control of a Large Gap 2-DOF Magnetic Bearing System on a Coupled Force Model, Proc. of the American Control Conf., Albuquerque, New Mexico, 1997.
15. Schoeb, R., Barletta, N. and Hahn, J., The Bearingless Centrifugal Pump - A Perfect Example of a Mechatronics System, 1st IFAC Conf. on Mechatronics Systems (Mechatronics 2000), Darmstadt, Sept. 2000.
16. Schoeb, R. et al, A Bearingless Motor for a Left Ventricular Assist Device, Proc. of the 7th Int. Symp. on Magnetic Bearings, ETH Zurich, August 2000.
17. Smith, R.D. and Weldon, W.F., Nonlinear Control of a Rigid Rotor Magnetic Bearing System: Modeling and Simulation with Full State Feedback, IEEE Trans. on Magnetics, Vol. 31, No. 2, Mar. 1995.
18. Vidyasagar, M., Nonlinear Systems Analysis, Prentice Hall, 1993.